

RESEARCH ARTICLE



Cite this: *RSC Med. Chem.*, 2021, 12, 1722

Peptidomimetic nitrile warheads as SARS-CoV-2 3CL protease inhibitors†

Bing Bai,^{ab} Elena Arutyunova,^{cd} Muhammad Bashir Khan,^c Jimmy Lu,^{id bd} Michael A. Joyce,^{id bd} Holly A. Saffran,^{bd} Justin A. Shields,^{id bd} Appan Srinivas Kandadai,^{ab} Alexandr Belovodskiy,^{id ab} Mostofa Hena,^{ab} Wayne Vuong,^e Tess Lamer,^{id e} Howard S. Young,^d John C. Vederas,^{id e} D. Lorne Tyrrell,^{abd} M. Joanne Lemieux^{id cd} and James A. Nieman^{id *ab}

Tragically, the death toll from the COVID-19 pandemic continues to rise, and with variants being observed around the globe new therapeutics, particularly direct-acting antivirals that are easily administered, are desperately needed. Studies targeting the SARS-CoV-2 3CL protease, which is critical for viral replication, with different peptidomimetics and warheads is an active area of research for development of potential drugs. To date, however, only a few publications have evaluated the nitrile warhead as a viral 3CL protease inhibitor, with only modest activity reported. This article describes our investigation of P3 4-methoxyindole peptidomimetic analogs with select P1 and P2 groups with a nitrile warhead that are potent inhibitors of SARS-CoV-2 3CL protease and demonstrate *in vitro* SARS-CoV-2 antiviral activity. A selectivity for SARS-CoV-2 3CL protease over human cathepsins B, S and L was also observed with the nitrile warhead, which was superior to that with the aldehyde warhead. A co-crystal structure with SARS-CoV-2 3CL protease and a reversibility study indicate that a reversible, thioimidate adduct is formed when the catalytic sulfur forms a covalent bond with the carbon of the nitrile. This effort also identified efflux as a property limiting antiviral activity of these compounds, and together with the positive attributes described these results provide insight for further drug development of novel nitrile peptidomimetics targeting SARS-CoV-2 3CL protease.

Received 22nd July 2021,
Accepted 20th August 2021

DOI: 10.1039/d1md00247c

rsc.li/medchem

Introduction

The outbreak of coronavirus disease 2019 (COVID-19) was first reported in December 2019 in Wuhan, China. To date, over 3.8 million people have died from this ongoing pandemic.¹ Although vaccines have been developed and are being administered as rapidly as possible, the emergence of variants has underscored the need for additional modalities of treatment. Remdesivir, which was originally in clinical trials as an Ebola treatment, is the only direct-acting antiviral

that has been approved.² It is administered intravenously and has demonstrated only modest efficacy for moderate cases of COVID-19.³ Novel therapeutics to treat coronavirus infections, especially ones with a different mechanism of action that are orally administered, are desperately needed.

COVID-19 is caused by a severe acute respiratory syndrome coronavirus-2 (SARS-CoV-2).¹ Other coronaviruses are responsible for a portion of common seasonal colds as well as the 2003 severe acute respiratory syndrome (SARS, caused by the SARS-CoV-1), and 2012 Middle East respiratory syndrome (MERS, caused by the MERS-CoV). Coronaviruses have four genera with two, the alpha- and beta-coronaviruses, descending from the bat viral gene pool with SARS-CoV-1, MERS-CoV and SARS-CoV-2 being beta-coronaviruses.⁴

During the replication cycle of the coronavirus, after endocytosis into the cell, cellular machinery is utilized to express two overlapping polyproteins, pp1a and pp1b, from the viral RNA.⁵ These polyproteins must be processed by two proteases known as 3-chymotrypsin-like protease (3CL^{pro}, M^{pro} or 3CLP) and papain-like protease (PL^{pro}) to liberate the viral proteins required for replication. The majority of the cleavages are performed by 3CL^{pro}, however, the exact number cleaved by each protease is still being debated.⁶ Both

^a Li Ka Shing Applied Virology Institute, University of Alberta, Edmonton, Alberta, T6G 2E1, Canada. E-mail: jnieman@ualberta.ca

^b Department of Medical Microbiology and Immunology, University of Alberta, Edmonton, Alberta, T6G 2E1, Canada

^c Department of Biochemistry, University of Alberta, Edmonton, Alberta, T6G 2H7, Canada

^d Li Ka Shing Institute of Virology, University of Alberta, Edmonton, Alberta, T6G 2E1, Canada

^e Department of Chemistry, University of Alberta, Edmonton, Alberta, T6G 2G2, Canada

† Electronic supplementary information (ESI) available. See DOI: 10.1039/d1md00247c

3CL^{Pro} and PL^{Pro} are cysteine proteases with different site specificities. The peptide sequence cleaved by a protease is labeled as P3P2P1↓P1'P2'P3' where the amide bond cleavage occurs between P1 and P1' amino acid as indicated by the arrow, and the corresponding sites on the protease protein are referred to as S3S2S1S1'S2'S3'. Coronavirus 3CL^{Pro} hydrolyses proteins predominantly between a P1 glutamine and a small P1' amino acid, such as alanine, serine or glycine. For the P2 position, leucine is the most common in the sequence specificity for coronaviruses.⁷ Given the importance of 3CL^{Pro} to viral replication, it is a promising drug target.

Peptidomimetic inhibitors of proteases mimic the substrate with similar labels (P3, P2, P1, *etc.*) and typically include a moiety that interacts with the catalytic site. That group is known as the warhead, and for cysteine proteases it is typically an electrophile that forms a covalent bond with the catalytic sulfur.⁵ The exploration of peptidomimetic inhibitors against SARS-CoV-2 3CL^{Pro} has unsurprisingly exploded since the COVID-19 pandemic began. Repurposing peptidomimetic drugs, such as boceprevir, telaprevir, and ritonavir, that were developed against other viruses is one approach that has been utilized.^{8–10} Peptidomimetics that are tailored for SARS-CoV-2 3CL^{Pro} are increasingly being reported, and many build upon SARS-CoV-1 findings or those of viruses that have a similar protease to the coronavirus 3CL^{Pro}, such as enterovirus 71 and rhinovirus.^{11–14} For these SARS-CoV-2 targeted peptidomimetics, most utilize a P1 glutamine mimic with a gamma-lactam (5-membered) being the most common, with *N,N*-dimethylglutamine, delta-lactam (6-membered) and non-glutamine mimics being less frequently reported. For P2, consistent with the consensus sequence, the most common utilized group is leucine, although related ones, such as cyclopropylalanine, *tert*-butylalanine and cyclohexylalanine, are also reported.^{11,14–22} The main variations being explored by different researchers are at either P3 or the warhead. A wide range of P3 capping groups, such as benzyl carbamate and indole, in addition to tetra- (P4) and pentapeptides (P4 and P5) with capping groups are utilized. The warhead is critical as it makes a covalent bond with the catalytic sulfur and must be reactive enough in the protease active site, but not too reactive to be sequestered by glutathione or indiscriminately react with other thiols. The warhead selection tends to differentiate the focus of investigators as different groups study distinct warheads and variations thereof. Recent SARS-CoV-2 targeted warheads that have been examined are: aldehydes and their prodrugs,^{14–16} ketoamides,^{11,17} halomethylketones,¹⁸ enoates,¹⁹ α -hydroxymethylketones²⁰ (HMK) and α -acyloxymethylketones (AMK).^{20–22} As the research into SARS-CoV-2 peptidomimetics matures, like prior HCV and HIV protease efforts, the structural elements will be adjusted to allow good pharmacokinetics and the ability to demonstrate *in vivo* efficacy. A noteworthy recent example was reported by Qiao *et al.* that found an aldehyde warhead

with the P2 leucine being replaced by a bicyclic proline (from HCV protease drug development) was able to demonstrate efficacy in a murine model of COVID-19 by intraperitoneal and oral administration.²³ Further research into understanding the roles the different moieties play in not only protease inhibition and anti-viral activity, but also other attributes, such as permeability, efflux, and metabolism, will allow inhibitors to be refined to discover drugs for the treatment of coronavirus infections. In addition, assessing selectivity for these peptidomimetics and their warheads for SARS-CoV-2 3CL^{Pro} over human cysteine proteases with a similar sequence specificity will be important to avoid potential toxicity; however, only a few articles include selectivity considerations.^{20,22,24}

To date no cysteine protease inhibitors for any indication have made it to regulatory approval.²⁵ Inspired by the clinical success of odanacatib (Fig. 1), a human cathepsin K inhibitor with a nitrile warhead, that progressed to phase III clinical trials, we decided to explore the nitrile group as a warhead on peptidomimetics to inhibit SARS-CoV-2 3CL^{Pro}.²⁶ A search of the literature in March 2020 for nitrile warhead utilization for 3CL^{Pro} inhibition produced only a couple of examples. These were against related enterovirus 71 and SARS-CoV-1,

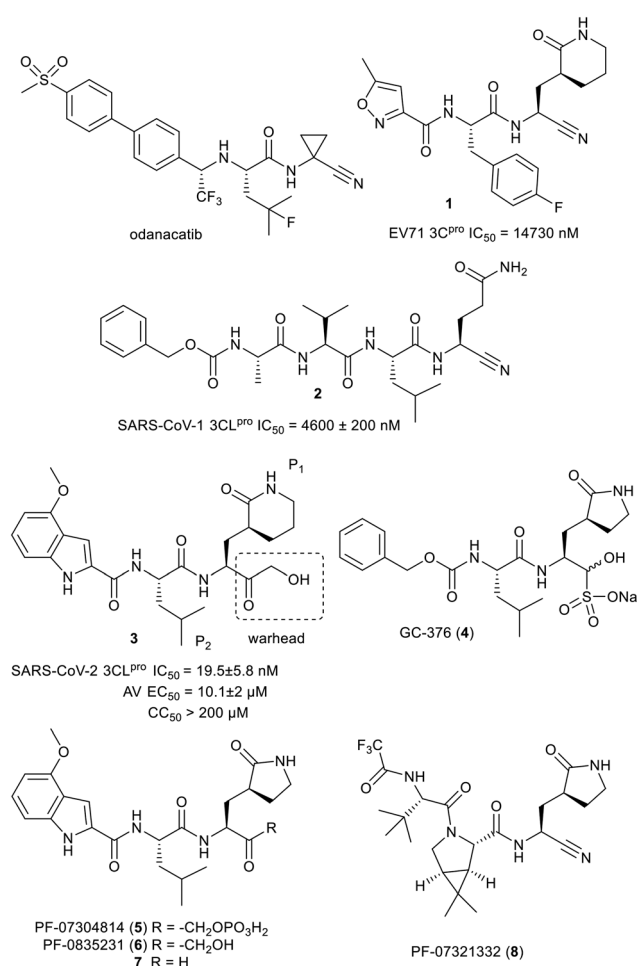


Fig. 1 Structures of odanacatib and compounds 1 to 8.

with all the compounds having at best either single or double digit micromolar IC_{50} values.^{27,28} Representative compounds **1** and **2** from those publications and their reported IC_{50} values are shown in Fig. 1. Undeterred by the high IC_{50} values we decided to examine nitrile analogs of an active compound **3** that was discovered upon screening compounds from our legacy norovirus protease program.

After our effort commenced, GC-376 (**4**) and PF-07304814 (**5**) were disclosed as SARS-CoV-2 3CL^{Pro} inhibitors that were under development to enter clinical trials to treat COVID-19.^{29,30,31}

Prodrug **5**, a more water soluble form of active compound **6**, is undergoing clinical trials as an intravenously administered drug.²⁰ Compound **6** and related compounds, such as aldehyde **7**, were initially disclosed in 2005 and 2006 and were some of the published sources of inspiration for our prior norovirus protease exploratory effort.^{32,33} In April 2021, a new potential COVID-19 treatment, PF-07321332 (**8**), targeting 3CL^{Pro} was disclosed by Pfizer and is reported to be dosed orally and has initiated clinical trials.³⁴ Compound **8** contains a nitrile warhead and to date we have observed no publication with its biological results. A recent literature search uncovered an investigation by Breidenbach *et al.* of a few tetra peptides with azaglutamine P1, nitrile warhead and benzylcarbamate capping group as a SARS-CoV-2 3CL^{Pro} inhibitors.³⁵ Other than the nitrile, these were structurally very different from our compounds and Breidenbach *et al.* only reported a modest k_{obs}/I and no antiviral data. Herein,

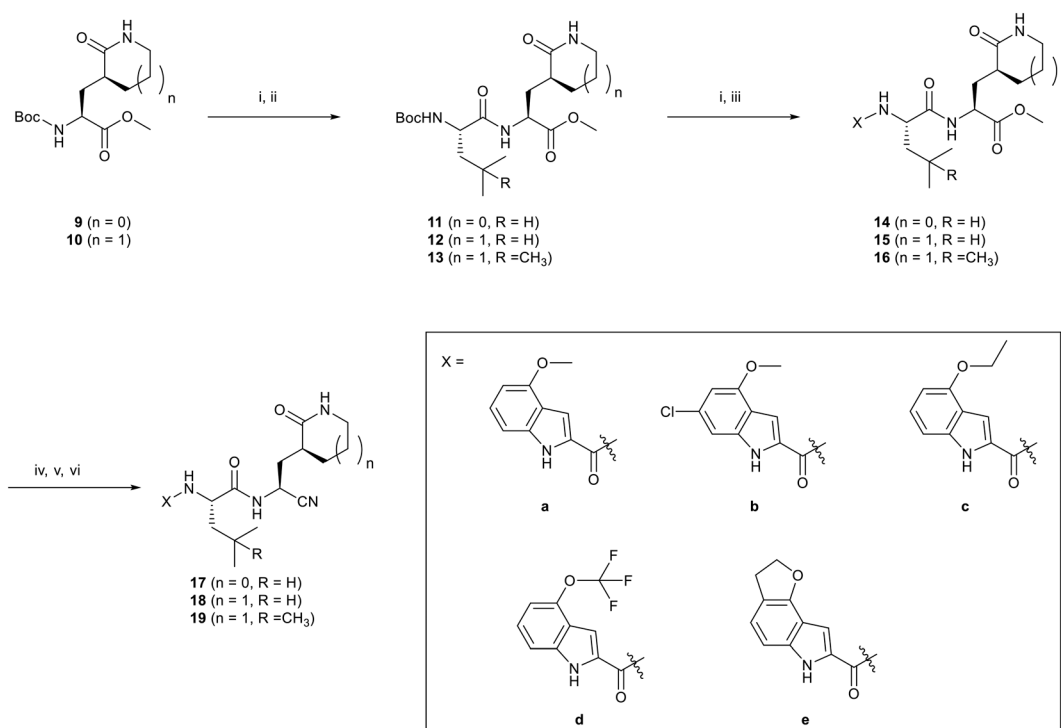
we report our results for nitrile warhead analogs of compound **3**, **6** and **7**.

Results

Chemistry

Compound **9** and **10** were prepared as described by Shang and coworkers.²⁷ Conversion of **9** to **11** and **10** to **13** (Scheme 1) followed literature procedures and **10** was converted to **13** using those sample protocols, but substituting *N*-(*tert*-butoxycarbonyl)-4-methyl-L-leucine for *N*-(*tert*-butoxycarbonyl)-L-leucine.^{36,37} Compound **11–13** were converted to the ester version of the target by removal of the *t*-butyl carbamate with HCl in a mixture of dioxane and dichloromethane followed by HATU coupling of the corresponding indol-2-ylcarboxylic acid (a to e). Conversion of the methyl ester to the nitrile target was achieved by a saponification with LiOH, then carbonyldiimidazole mediated coupling of ammonia and dehydration of the primary amide with trifluoroacetic acid anhydride.

Late stage diversification is always preferred to generate the same number of targets in fewer overall steps. The nitrile version of **10** proved challenging to efficiently generate, deprotect and couple to *N*-*t*-Boc-L-leucine producing low yields of impure material. The route in Scheme 1 was thus employed for compound production, despite the added number of steps required.



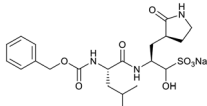
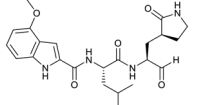
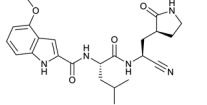
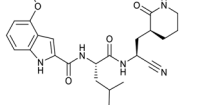
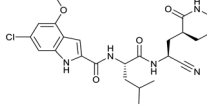
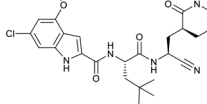
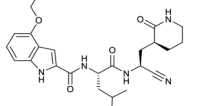
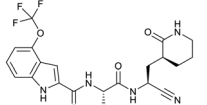
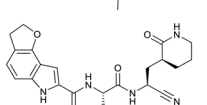
Scheme 1 Synthesis of compounds. i) TFA in DCM or HCl in dioxane, DCM ii) *N*-(*tert*-butoxycarbonyl)-L-leucine ($R = H$) or *N*-(*tert*-butoxycarbonyl)-4-methyl-L-leucine ($R = CH_3$), HATU, NMM or Et₃N, DMF, 94% yield (2 steps, $R = H$), 91% yield (2 steps, $R = CH_3$); iii) corresponding (a–e) indolecarboxylic acid, HATU, NMM or Et₃N, DMF, 30–98% yield (2 steps); iv) LiOH, THF, v) CDI, THF, NH₃·H₂O; vi) trifluoroacetic acid anhydride, Et₃N, THF, 0 °C, 12–63% yield (3 steps).

Biology

Studies by a subset of authors of this manuscript reported last year the discovery that GC-376 (**4** in Fig. 1), which is an aldehyde prodrug, displayed good SARS-CoV-2 3CL^{pro} and antiviral activity.²⁹ Exploring the structure–activity relationship of the aldehyde and bisulfate derivatives generated a series of compounds, including **7** (Fig. 1), that showed better inhibition of SARS-CoV-2 3CL^{pro}, although similar antiviral activity was obtained.^{15,38} For this study we wanted to explore the utility of the nitrile warhead with the

gamma- versus delta-lactam in P1, and examine different indole substituents with the more active P1. The same protocols were used as detailed previously, see also ESI.†²⁹ In Table 1, the SARS-CoV-2 3CL^{pro} FRET inhibition results are shown for our peptidomimetics with a nitrile warhead in comparison to **4** and **7**. Compound **17a**, which is the nitrile analog of **7**, showed a comparable IC₅₀ value to aldehyde **7** against SARS-CoV-2 3CL^{pro}, but was considerably more active than **4**. The α -hydroxymethylketone (HMK) **6** (Fig. 1) had an IC₅₀ value of 18.9 nM in this FRET assay. The IC₅₀ values for SARS-CoV-2 3CL^{pro} of **6**, **7** and **17a** were only a few-fold of

Table 1 Results for protease inhibition and SARS-CoV-2 plaque reduction for compounds

Cmpd	Structure	SARS-CoV-2 3CL ^{pro} IC ₅₀ ^a (nM)	EC ₅₀ PRA ^b (μ M)	EC ₅₀ PRA + CP ^c (μ M)	Inhibition at 1 μ M and/or ^d [IC ₅₀ in nM]		
					Human CatB	Human CatS	Human CatL
4		190 \pm 40	0.9 \pm 0.2	0.25 \pm 0.02	53% [1400 \pm 10]	99% [23 \pm 3]	100% [0.25 \pm 0.08]
7		60 \pm 10	0.9 \pm 0.1	0.25 \pm 0.01	NR [2000 \pm 700]	NR [40 \pm 10]	53% [280 \pm 60]
17a		40 \pm 8	>5	NR	<1% [28 000 \pm 8000]	78% [700 \pm 100]	15% [1450 \pm 300]
18a		13 \pm 3	2.7 \pm 0.7	0.23 \pm 0.04	<1% [32 000 \pm 7000]	73% [2500 \pm 500]	22% [640 \pm 050]
18b		9.1 \pm 2.5	2.2 \pm 0.5	0.233 \pm 0.007	<1% [18 000 \pm 3000]	72% [400 \pm 80]	37% [470 \pm 80]
19b		14 \pm 2	1.5 \pm 0.4	0.21 \pm 0.05	<1%	64%	18%
18c		24 \pm 4	4.8 \pm 0.5	0.12 \pm 0.04	<1%	74%	<1%
18d		13.7 \pm 1.5	2.6 \pm 0.3	0.35 \pm 0.09	<1%	67%	8%
18e		49 \pm 10	>10	NR	<1%	67%	10%

^a – See ESI,† determined from 8 concentrations performed in triplicate. ^b – Determined from 6 concentrations performed in at least triplicate (Vero E6 host cells); CC₅₀ of all compounds (except **18d**) was >200 μ M (Vero E6 and A549). ^c – Same as b, but all wells contain 0.5 μ M CP-100356. ^d – Run in duplicate or triplicate and at least 6 concentrations were utilized to determine IC₅₀ values. NR – not run.

each other with HMK appearing slightly more active. Replacing the gamma-lactam in **17a** with its 6-membered homologue (compound **18a**) provided a slight increase in inhibition reducing the IC₅₀ value to 13 nM for SARS-CoV-2 3CL^{pro}. An IC₅₀ value of 19.5 nM was obtained for the HMK analogue **3** (Fig. 1), which is similar to **18a** reinforcing the observation that the peptidomimetics with the nitrile and HMK warheads show comparable inhibition towards SARS-CoV-2 3CL^{pro}.

Based on a crystal structure obtained (*vide infra*) there appeared to be room available to further substitute the indole, and with **18a** showing slightly better activity we decided to maintain the delta-lactam in P1 while exploring additional variations. The 6-chlorosubstitution, **18b**, produced a similar, although possibly slightly improved inhibition of SARS-CoV-2 3CL^{pro} compared to **18a**. The *t*-butylalanine P2 version, **19b**, produced inhibition in the same range as **18a** and **18b**, suggesting no activity benefit compared to P2 leucine. Utilizing a 4-ethoxy (**18c**) instead of 4-methoxy (**18a**) appears to result in a slightly reduced inhibition. The IC₅₀ values for the trifluoromethyl (**18d**) and methyl (**18a**) ethers were virtually identical. The 4,5-dihydrofurano-fused indole **18e** lost activity compared to both the methoxy and ethoxy versions, **18a** and **18c**.

To confirm the compounds were not cytotoxic, viability determinations were carried out on all **17–19** compounds using both CellTiter Glo and CCK8 readouts with both Vero E6 and A549 cells and all the compounds displayed a CC₅₀ value greater than 200 μM in all 4 assays, except **18d**. The outlier, **18d**, had a CC₅₀ of >100 μM against Vero E6 and against the more sensitive A549 cells had a CC₅₀ value of approximately 90 μM. Compound **4** and **7** were reported previously and had CC₅₀ values of greater than 200 μM.¹⁵

Compounds **17–19** were examined in a SARS-CoV-2 plaque reduction assay (PRA) using Vero E6 host cells (Table 1). They were initially screened for their antiviral activity at 10 μM and if 3-fold or greater reduction in plaques was observed for a compound it was tested in a concentration response curve to determine the EC₅₀ value. If less than 2-fold reduction was observed the compound was assigned >10 μM, and if less than a 3-fold reduction was observed at 10 μM then >5 μM was assigned. Compounds **18a**, **18b**, **18c**, **19b** and **18d** had low single digit micromolar EC₅₀ values in the PRA. Compared to compound **4** and **7**, these 5 compounds had lower IC₅₀ values against SARS-CoV-2 3CL^{pro}, but higher EC₅₀ values in the PRA. One possible rationale is that these nitriles are more susceptible to efflux than structurally related **7**, which is a recognised consideration for Vero cells.³⁹ To determine if these compounds were undergoing efflux we repeated the PRA assay in the presence of a known efflux inhibitor CP-100356 (CP) at 0.5 μM to determine the extent of efflux (Table 1).^{20,40} As reported previously, the EC₅₀ values for **4** and **7** decreased about 3-fold indicating some active transport out of the cell.¹⁵ For compounds **18a**, **18b**, **19b**, **18c**, and **18d**, inhibiting efflux with CP in the PRA resulted in approximately a 10-fold improvement in their anti-viral

activity resulting in EC₅₀ values similar to **4** and **7** in the presence of CP. This strongly suggests that efflux plays a role in the higher EC₅₀ values for these nitrile compounds in the absence of CP.

As these nitrile inhibitors demonstrated SARS-CoV-2 3CL^{pro} inhibition and *in vitro* SARS-CoV-2 antiviral activity, we decided to examine their reactivity and selectivity. Some reactive warheads are susceptible to reaction with glutathione (GSH) and so we decided to test if GSH sequesters these nitrile inhibitors. We incubated **18a** with GSH (10 mM) at pH 7.4 at 37 °C for 24 h and observed equally high recovery (≥90%) of **18a** to one incubated in the phosphate buffer without GSH. The high recovery of **18a** and lack of observed glutathione adduct (by LC/MS) demonstrate these nitrile warheads are stable in the presence of high levels of GSH, or that any reaction is readily reversible. We then turned our attention to selectivity over human cysteine proteases that have a similar sequence specificity for P2 and P1, leucine and glutamine, respectively. These are more likely to prove challenging to obtain selectivity over than a protease with a different catalytic mechanism and substrate specificity. The human cysteine proteases cathepsin B (CatB), cathepsin S (CatS) and cathepsin L (CatL) have similar specificities in P2 and P1 as SARS-CoV-2 3CL^{pro}.⁴¹ Cathepsins are involved in numerous physiological and pathological processes and are themselves potential drug targets as they have suspected roles in numerous human diseases.⁴¹

To compare selectivity of another warhead we decided to also examine **4** and **7** for their ability to inhibit CatB, S and L. As the bisulfite adduct formed in **4** is reversible, both these compounds utilize aldehyde warheads.¹⁵ Both **4** and **7** were less potent inhibitors of CatB than CatS. The CatS IC₅₀ values were 23 nM and 40 nM, respectively, which indicate that these two aldehyde warhead compounds show no selectivity for SARS-CoV-2 3CL^{pro}. Compound **4** was 8-fold more active against CatS than SARS-CoV-2 3CL^{pro}. The extremely potent inhibition of CatL by **4**, with an IC₅₀ value of 0.25 nM, was consistent with the recently reported value of 0.33 nM.²⁴ Compound **7** was 1120-fold less active against CatL than **4**, indicating a significant influence of the 4-methoxyindol-2-yl *versus* benzyloxy P3 groups. Compound **7** was, however, still less than 5-fold more selective for SARS-CoV-2 3CL^{pro} than CatL.

All the nitriles **17–19** displayed low inhibition of CatB when screened at 1 μM, while CatS and CatL showed inhibition at that concentration (Table 1). Concentration response curves were obtained for select compounds to compare with the IC₅₀ values obtained for **4** and **7**. Comparing **7** to **17a**, where the only change is the warhead, indicates that the nitrile warhead is over 10 times less active against CatB and CatS than the aldehyde warhead. Although for CatL the difference is reduced, the nitrile analog is still 5-fold less active compared to the aldehyde. This resulted in nitrile **17a** displaying a significantly better selectivity for SARS-CoV-2 3CL^{pro} over the human cathepsins B, S and L than aldehyde **7**.

Comparison of the gamma- and delta-lactam, **17a** and **18a**, showed the IC₅₀ value against CatB was within error for both, while for CatS **18a** was a few-fold less active than **17a** and for CatL the reverse was the case. With **18a** having a low IC₅₀ value for SARS-CoV-2 3CL^{pro}, this compound obtained excellent selectivity over CatB and CatS of 2424-fold and 189-fold, respectively, and reasonable selectivity over CatL of 48-fold. The compound with the lowest IC₅₀ value against SARS-CoV-2 3CL^{pro}, **18b**, also had increased inhibition of CatB, CatS and CatL in relation to **17a** and **18a**. Regardless, compared to **4** and **7**, **18b** still showed better selectivity for SARS-CoV-2 3CL^{pro} over CatB, CatS and CatL than the aldehyde warhead containing peptidomimetics.

To determine the nature of the inhibition a reversibility study was done with **18a** (Fig. 2). The dialysis of inhibited 3CL^{pro} resulted in an increase of enzymatic activity over time, which is indicative of reversible binding of the inhibitor. We observed a recovery of 10% of activity after only 4 hours, and a 45% recovery of initial activity after 3 days. The enzyme 3CL^{pro} loses activity overtime and the intersection of recovery of activity and loss of enzymatic activity is approximately 65 h for **18a**. This recovery of activity as **18a** is dialyzed away demonstrates the reversible nature of the inhibition of this nitrile warhead.

An initial structure of SARS-CoV-2 3CL^{pro} was solved by Zhang *et al.*¹¹ The structure of **17a** with SARS-CoV2 3CL^{pro} was determined by molecular replacement, using the crystal structure of the free enzyme of the SARS-CoV-2 3CL^{pro} (PDB entry 6WTM)²⁹ as a search model. The structure obtained had a resolution of 2.15 Å and is shown in Fig. 3 (PDB: 7R7H). It crystalized as a dimer, and the active site of both protomers contained **17a** bound in a very similar orientation. The nitrile reacted with the catalytic sulfur of Cys145 to generate a thioimidate adduct. This is a reversible process as seen in Fig. 2. This thioimidate has similar bond lengths, 1.8 Å C–S bond length, and geometries, sp² carbon, to that observed with other cysteine proteases with nitrile warheads, such as odanacatib – cathepsin K complex (PDB: 5TDI). For both SARS-CoV-2 3CL^{pro}-**17a** protomers the imine nitrogen of the thioimidate moiety is within hydrogen bonding distance of the NH for both Cys145 and Gly143, 3.3 Å and 3.4 Å, respectively for chain A, with 3.2 Å and 3.7 Å for chain B. The

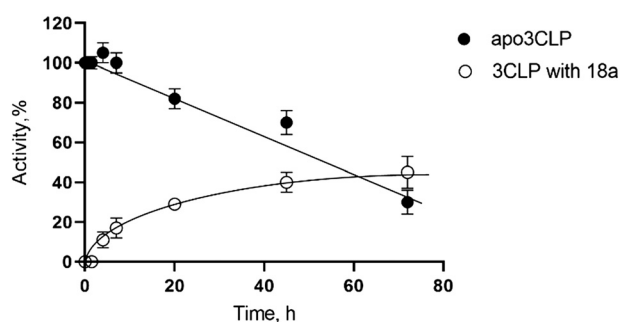


Fig. 2 Activity of SARS-CoV-2 3CL^{pro} over time in media or after exposure to **18a** (reversibility experiment).

rest of the hydrogen bonding network is practically identical to that seen previously for aldehyde **7** and HMK **6** (PDB: 7LDL and 6XHM, respectively).^{15,20}

Discussion

Despite the previous modest results against viral cysteine proteases in the literature, the nitrile warhead with improved peptidomimetic groups demonstrated potent SARS-CoV-2 3CL^{pro} inhibition. The inhibition of SARS-CoV-2 3CL^{pro} for the nitrile warhead containing peptidomimetic was similar to the corresponding aldehyde analog, comparing IC₅₀ values of **17a** to **7** (Table 1).

The delta-lactam had a lower IC₅₀ than the gamma-lactam, **17a** to **18a**, which is consistent to Shang, Yin and coworkers observation for enterovirus-71 3C protease with an aldehyde warhead.²⁷ It is worth noting that no difference in IC₅₀ values for the gamma- and delta-lactams in P1 against SARS-CoV-2 3CL^{pro} was observed in our previous study with an AMK warhead.²² Further studies with different warheads and proteases will be required to understand the factors influencing the activity of the delta-lactam compared to the gamma-lactam. In addition, the selectivity differences, such as seen in Table 1, and other attributes, such as pharmacokinetic properties, will also need to be evaluated to select the optimal lactam group.

Fig. 3 shows the co-crystal structure for SARS-CoV-2 3CL^{pro}-**17a** that we obtained indicating that a covalent bond is formed between the sulfur of Cys145 and the nitrile generating a thioimidate adduct. Based on reversibility studies this is a reversible, covalent adduct. That structure did not reveal any close contacts around the end of the capping group (Fig. 3) suggesting the opportunity to add substituents on the phenyl or methoxy of the 4-methoxyindole. However, only the 6-chloro derivative **18b** displayed a possibly modest increase in protease inhibition compared to **18a**, but resulted in slightly lower selectivity attributes over CatB and CatS compared to the same compound. Other substitutions tested did not prove advantageous as the trifluoromethoxy group (**18d**) displayed toxicity (CC₅₀ < 200 μM) and the ethoxy (**18c**) and dihydrofurano (**18e**) derivatives lost activity against SARS-CoV-2 3CL^{pro} as well as in the antiviral assay.

All the nitrile analogs (**17–19**) have IC₅₀ values less than 100 nM for SARS-CoV-2 3CL^{pro} inhibition, but only those with values less than 25 nM showed an EC₅₀ value of less than 5 μM in the PRA. Aldehydes **4** and **7** were both more active in the PRA. The nitrile analogs all had an approximately 10-fold reduction of EC₅₀ value when the efflux inhibitor CP was added, suggesting that these peptidomimetic compounds were undergoing significant efflux from Vero E6 cells. Structural alterations to improve properties, such as H-bond donor removal and other depeptidization strategies could improve properties and overcome the efflux issue.⁴²

Compound **4** demonstrated extremely potent inhibition of CatL, which was consistent with that recently reported in the

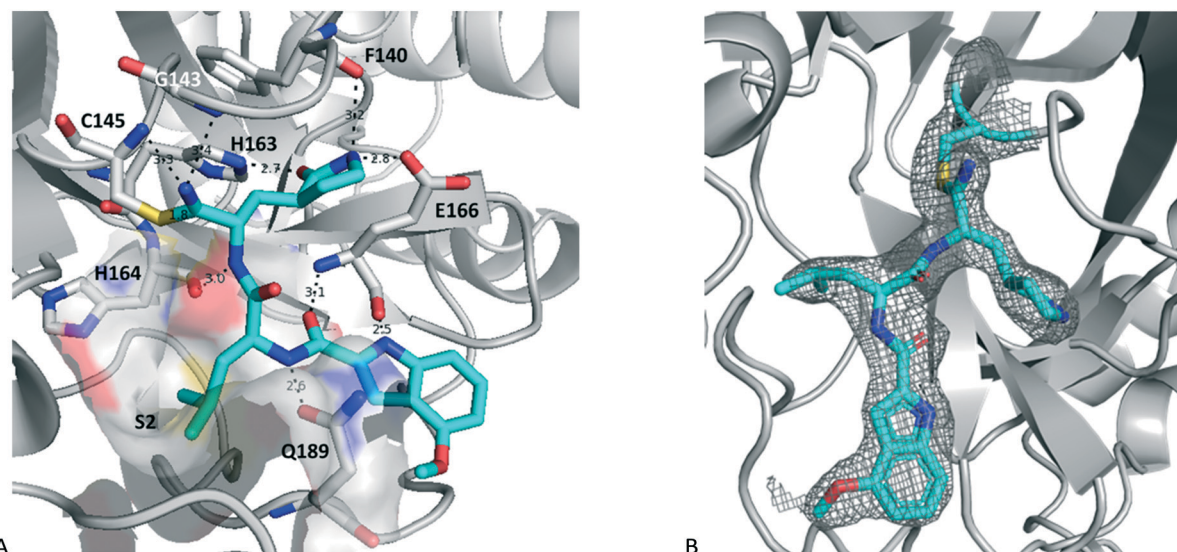


Fig. 3 Structure of **17a** bound to SARS-CoV-2 3CL^{Pro} (PDB entry 7R7H) with A showing the hydrogen bonding network, S2 pocket and thioimide (chain A) and B showing the electron density of the ligand (chain B).

literature.²⁴ Compound **4** also had almost 10-fold higher inhibition of CatS than SARS-CoV-2 3CL^{Pro}. For CatL, the P3 capping group made a substantial difference when comparing **7** to **4**, but only a modest difference was observed for CatS (Table 1).

All compounds in Table 1 were more selective for SARS-CoV-2 3CL^{Pro} than for CatB, with the nitriles **17a**, **18a** and **18b** having >1000-fold selectivity. These compounds, **17a**, **18a** and **18b**, also showed lower inhibition of CatS and CatL than aldehydes **4** and **7** and superior selectivity for SARS-CoV-2 3CL^{Pro}. Literature IC₅₀ values for HMK **6** for CatB and CatL inhibition are 1.3 μM and 146 nM, respectively.^{20,24} Comparison of these values to the nitrile analog **17a** (Table 1) for CatB and CatL suggests that the nitrile warhead is significantly less active at inhibiting these cathepsins than the HMK warhead (*ca.* 21- and 10-fold less), although a head-to-head comparison is required to confirm this higher selectivity. The selectivity criteria required for a drug still needs to be established. For example, CatS drugs in clinical trials were well-tolerated in healthy volunteers, but did show an increased respiratory tract infection rate in a small percentage of patients making potent CatS inhibition a concern for COVID-19 therapy.⁴³ CatL activity is implicated in being important to the SARS-CoV-2 replication cycle, such as spike protein processing and possibly exit from cells, and its inhibition could also be a mechanism to inhibit viral replication.^{44,45,46} CatS and CatL are important lysosomal endopeptidase enzymes and further research is needed to understand the level of selectivity that is required to avoid side-effects *in vivo*.

The results herein demonstrate that these nitrile warhead containing peptidomimetics have good potency against SARS-CoV-2 3CL^{Pro} and display selectivity over human cysteine proteases (CatB, CatS and CatL) that have overlapping sequence specificity for P2 and P1. Further structural

alterations to reduce efflux, for example by removing peptide character, is currently being investigated. The structure of Pfizer's recently revealed oral clinical candidate with a nitrile warhead (**8** in Fig. 1) demonstrates one method that this can be successfully achieved, and alternate approaches could yield diverse oral SARS-CoV-2 3CL^{Pro} therapies with different favourable attributes, such as maintaining activity against clinically relevant SARS-CoV-2 3CL^{Pro} mutants.⁴⁷ Continued research on this promising target and these peptidomimetics has the potential to add to the arsenal of direct-acting antivirals needed to combat the current COVID-19 pandemic, emerging variants and future coronavirus outbreaks.

Conclusions

Direct-acting antivirals to treat COVID-19 are desperately needed and the viral encoded protein 3CL^{Pro}, which is a cysteine protease required for viral replication, is a promising drug target. Treatment of proteases typically utilize peptidomimetics that mimic the substrate and this article demonstrated that a nitrile warhead provides compounds with good SARS-CoV-2 3CL^{Pro} inhibition and selectivity over human cysteine proteases (CatB, CatS and CatL) with overlapping sequence specificity in P1 and P2. For the same peptidomimetic, the nitrile warhead demonstrated superior activity (lower IC₅₀) against SARS-CoV-2 3CL^{Pro} and greater selectivity over human CatB, CatS and CatL than the aldehyde warhead analog. Some nitrile warhead analogs with a P1 delta-lactam also displayed EC₅₀ values of 1–3 micromolar in a SARS-CoV-2 plaque reduction assay, with CC₅₀ values of greater than 200 μM. Efflux appears to be an issue for these compounds and reducing the susceptibility of active transport of future nitrile warhead containing analogs, such as by removing peptide character, has the potential to improve both antiviral activity and generate favourable

properties to enable development of novel oral therapeutics to treat COVID-19.

Author contributions

Authors that contributed to investigation and methodology are BB, EA, MJL, MBK, MAJ, HAS, JAS, ASK, AB, MH, and WV. BB, JL, ASK, WV and TL contributed to resources. Visualization was performed by EA, MBK, MAJ, MJL and JAN. The authors that supervised were HSY, JCV, DLT, MAJ, MJL and JAN. Funding acquisition and project administration were by MJL, DLT and JAN. JAN wrote the original draft and all authors reviewed the manuscript prior to publication.

Conflicts of interest

There are no conflicts to declare.

Acknowledgements

The authors would like to thank numerous colleagues at the University of Alberta including: Vishwa Somayaji (Faculty of Pharmacy and Pharmaceutical Sciences) for running ^1H , ^{13}C and ^{19}F NMRs; Jack Moore (Alberta Proteomics and Mass Spectrometry Facility) for HRMS; Wayne Moffat and Madison Gauthier (Department of Chemistry) for IR. We thank the staff at SSRL beamline 12-1, in particular Dr. Silvia Russi and Lisa Dunn. Use of the Stanford Synchrotron Radiation Lightsource, SLAC National Accelerator Laboratory, is supported by the U.S. Department of Energy, Office of Science, Office of Basic Energy Sciences under Contract No. DE-AC02-76SF00515. The SSRL Structural Molecular Biology Program is supported by the DOE Office of Biological and Environmental Research, and by the National Institutes of Health, National Institute of General Medical Sciences (P30GM133894). The contents of this publication are solely the responsibility of the authors and do not necessarily represent the official views of NIGMS or NIH. Funding for the project were provided by Alberta Innovates (RES27408) and Canadian Institutes of Health Research Rapid Research (VR3-172655).

Notes and references

- 1 World Health Organization, <http://www.who.int/emergencies/diseases/novel-coronavirus-2019>, (accessed June 14, 2021).
- 2 J. Pardo, A. M. Shukla, G. Chamarthi and A. Gupte, *Drugs Context*, 2020, **9**, 1–9.
- 3 US Food and Drug Administration, <https://www.fda.gov/news-events/press-announcements/fda-approves-first-treatment-covid-19>, (accessed February 6, 2021).
- 4 S. K. P. Lau, P. Lee, A. K. L. Tsang, C. C. Y. Yip, H. Tse, R. A. Lee, L.-Y. So, Y.-L. Lau, K.-H. Chan, P. C. Y. Woo and K.-Y. Yuen, *J. Virol.*, 2011, **85**(21), 11325–11337; Centers for Disease Control and Prevention, <https://www.cdc.gov/coronavirus/types.html>, (accessed February 6, 2021); V. Anirudhan, H. Lee, H. Cheng, L. Cooper and L. Rong, *J. Med. Virol.*, 2021, **93**(5), 1–13.
- 5 H. Yang and J. Yang, *RSC Med. Chem.*, 2021, **12**, 1026–1036.
- 6 S. Yan and G. Wu, *FASEB J.*, 2021, **35**, e21573.
- 7 M. Xiong, H. Su, W. Zhao, H. Xie, Q. Shao and Y. Xu, *Med. Res. Rev.*, 2020, **41**(4), 1–34.
- 8 R. Oerlemans, A. J. Ruiz-Moreno, Y. Cong, N. D. Kumar, D. A. Velasco-Velazquez, C. G. Neochoritis, J. Smith, F. Reggiori, M. R. Grovesa and A. Dömling, *RSC Med. Chem.*, 2021, **12**, 370–379.
- 9 M. Mahdi, J. A. Mótyán, Z. I. Szojka, M. Golda, M. Miczi and J. Tózsér, *Virolog. J.*, 2020, **17**, 190.
- 10 A. Citarella, A. Scala, A. Piperno and N. Micale, *Biomolecules*, 2021, **11**, 607.
- 11 L. Zhang, D. Lin, X. Sun, U. Curth, C. Drosten, L. Sauerhering, S. Becker, K. Rox and R. Hilgenfeld, *Science*, 2020, **368**, 409–412.
- 12 T. Pillaiyar, M. Manickam, V. Namasivayam, Y. Hayashi and S.-H. Jung, *J. Med. Chem.*, 2016, **59**, 6595–6628.
- 13 W. Cui, K. Yang and H. Yang, *Front. Mol. Biosci.*, 2020, **7**, 616341.
- 14 W. Dai, B. Zhang, X.-M. Jiang, H. Su, J. Li, Y. Zhao, X. Xie, Z. Jin, J. Peng, F. Liu, C. Li, Y. Li, F. Bai, H. Wang, X. Cheng, X. Cen, S. Hu, X. Yang, J. Wang, X. Liu, G. Xiao, H. Jiang, Z. Rao, L.-K. Zhang, Y. Xu, H. Yang and H. Liu, *Science*, 2020, **368**, 1331–1335.
- 15 W. Vuong, C. Fischer, M. J. van Belkum, T. Lamer, K. D. Willoughby, M. B. Khan, E. Arutyunova, M. A. Joyce, H. A. Saffran, J. A. Shields, H. S. Young, J. A. Nieman, D. L. Tyrrell, M. J. Lemieux and J. C. Vederas, *Eur. J. Med. Chem.*, 2021, **222**, 113584.
- 16 C. S. Dampalla, Y. Kim, N. Bickmeier, A. D. Rathnayake, H. N. Nguyen, J. Zheng, M. M. Kashipathy, M. A. Baird, K. P. Battaile, S. Lovell, S. Perlman, K.-O. Chang and W. C. Groutas, *J. Med. Chem.*, 2021, **64**(14), 10047–10058.
- 17 L. Zhang, D. Lin, Y. Kusov, Y. Nian, Q. Ma, J. Wang, A. von Brunn, P. Leyssen, K. Lanko, J. Neyts, A. de Wilde, E. J. Snijder, H. Liu and R. Hilgenfeld, *J. Med. Chem.*, 2020, **63**(9), 4562–4578.
- 18 W. Zhu, M. Xu, C. Z. Chen, H. Guo, M. Shen, X. Hu, P. Shinn, C. Klumpp-Thomas, S. G. Michael and W. Zheng, *ACS Pharmacol. Transl. Sci.*, 2020, **3**, 1008–1016.
- 19 Z. Jin, X. Du and Y. Xu, *Nature*, 2020, **582**(7811), 289–293.
- 20 R. L. Hoffman, R. S. Kania, M. A. Brothers, J. F. Davies, R. A. Ferre, K. S. Gajiwala, M. He, R. J. Hogan, K. Kozminski, L. Y. Li, J. W. Lockner, J. Lou, M. T. Marra, L. J. Mitchell Jr., B. W. Murray, J. A. Nieman, S. Noell, S. P. Planken, T. Rowe, K. Ryan, G. J. Smith III, J. E. Solowiej, C. M. Steppan and B. Taggart, *J. Med. Chem.*, 2020, **63**, 12725–12747.
- 21 M. A. T. van de Plassche, M. Barniol-Xicotá and S. H. L. Verhelst, *ChemBioChem*, 2020, **21**, 3383–3388.
- 22 B. Bai, A. Belovodskiy, M. Hena, A. S. Kandadai, M. A. Joyce, H. A. Saffran, J. A. Shields, M. B. Khan, E. Arutyunova, J. Lu, S. K. Bajwa, D. Hockman, C. Fischer, T. Lamer, W. Vuong, M. J. van Belkum, Z. Gu, F. Lin, Y. Du, J. Xu, M. Rahim, H. S. Young, J. C. Vederas, D. L. Tyrrell, M. J. Lemieux and J. A. Nieman, *J. Med. Chem.*, 2021, DOI: 10.1021/acs.jmedchem.1c00616.

- 23 J. Qiao, Y.-S. Li, R. Zeng, F.-L. Liu, R.-H. Luo, C. Huang, Y.-F. Wang, J. Zhang, B. Quan, C. Shen, X. Mao, X. Liu, W. Sun, W. Yang, X. Ni, K. Wang, L. Xu, Z.-L. Duan, Q.-C. Zou, H.-L. Zhang, W. Qu, Y.-H.-P. Long, M.-H. Li, R.-C. Yang, X. Liu, J. You, Y. Zhou, R. Yao, W.-P. Li, J.-M. Liu, P. Chen, Y. Liu, G.-F. Lin, X. Yang, J. Zou, L. Li, Y. Hu, G.-W. Lu, W.-M. Li, Y.-Q. Wei, Y.-T. Zheng, J. Lei and S. Yang, *Science*, 2021, **371**, 1374–1378.
- 24 K. Vandyck, R. Abdelnabi, K. Gupta, D. Jochmans, A. Jekle, J. Deval, D. Misner, D. Bardiot, C. S. Foo, C. Liu, S. Ren, L. Beigelman, L. M. Blatt, S. Boland, L. Vangeel, S. Dejonghe, P. Chaltin, A. Marchand, A. Serebryany, A. Stoycheva, S. Chanda, J. A. Symons, P. Raboisson and J. Neyts, *Biochem. Biophys. Res. Comm.*, 2021, **555**, 134–139.
- 25 (a) B. Turk, *Nat. Rev. Drug Discovery*, 2006, **5**, 785–799; (b) Y. Hamada and Y. Kiso, *Biopolymers*, 2016, **106**, 563–579.
- 26 M. R. McClung, M. L. O'Donoghue, S. E. Papapoulos, H. Bone, B. Langdahl, K. G. Saag, I. R. Reid, D. P. Kiel, I. Cavallari, M. P. Bonaca, S. D. Wiviott, T. de Villiers, X. Ling, K. Lippuner, T. Nakamura, J.-Y. Reginster, J. A. Rodriguez-Portales, C. Roux, J. Zanchetta, C. A. F. Zerbin, J.-G. Park, K. Im, A. Cange, L. T. Grip, N. Heyden, C. DaSilva, D. Cohn, R. Massaad, B. B. Scott, N. Verbruggen, D. Gurner, D. L. Miller, M. L. Blair, A. B. Polis, S. A. Stoch, A. Santora, A. Lombardi, A. T. Leung, K. D. Kaufman and M. S. Sabatine, *Lancet*, 2019, **7**(12), 899–911.
- 27 Y. Zhai, X. Zhao, Z. Cui, M. Wang, Y. Wang, L. Li, Q. Sun, X. Yang, D. Zeng, Y. Liu, Y. Sun, Z. Lou, L. Shang and Z. Yin, *J. Med. Chem.*, 2015, **58**, 9414–9420; Y. Wang, L. Cao, Y. Zhai, J. Ma, Q. Nie, T. Li, A. Yin, Y. Sun and L. Shang, *Antiviral Res.*, 2017, **121**, 91–100.
- 28 C.-P. Chuck, C. Chen, Z. Ke, D. C.-C. Wan, H.-K. Chow and K.-B. Wong, *Eur. J. Med. Chem.*, 2013, **59**, 1–6.
- 29 W. Vuong, M. B. Khan, C. Fischer, E. Arutyunova, T. Lamer, J. Shields, H. A. Saffran, R. T. McKay, M. J. van Belkum, M. A. Joyce, H. S. Young, D. L. Tyrrell, J. C. Vederas and M. J. Lemieux, *Nat. Commun.*, 2020, **11**, 4282.
- 30 Anivive Repurposes Veterinary Drug GC376 for COVID-19 And Submits Pre-IND to FDA, PRNewswire Press release May 26, 2020, Anivive Lifesciences Inc.; K. Vandyck and J. Deval, *Curr. Opin. Virol.*, 2021, **49**, 36–40.
- 31 B. Halford, *Pfizer's novel COVID-19 antiviral heads to clinical trials*, C&EN, 2020, vol. 98(37), p. 9.
- 32 R. L. Hoffman, R. S. Kania, J. A. Nieman, S. P. Planken and G. J. Smith, WO2005/113580, 2005.
- 33 R. S. Kania, L. J. Mitchell and J. A. Nieman, WO2006/061714, 2006.
- 34 B. Halford, *Pfizer unveils its oral SARS-CoV-2 inhibitor*, C&EN, 2021, vol. 99(13), p. 7; E. Dolgin, *Nature*, 2021, **592**, 340–343.
- 35 J. Breidenbach, C. Lemke, T. Pillaiyar, L. Schäkel, G. Al Hamwi, M. Dieltz, R. Gedschold, N. Geiger, V. Lopez, S. Mirza, V. Namasivayam, A. C. Schiedel, K. Sylvester, D. Thimm, C. Vielmuth, L. P. Vu, M. Zylina, J. Bodem, M. Gütschow and C. E. Müller, *Angew. Chem., Int. Ed.*, 2021, **60**, 10423–10429.
- 36 A. M. Priora, Y. Kimb, S. Weerasekara, M. Morozea, K. R. Alliston, R. A. Z. Uy, W. Groutas, K.-O. Chang and D. H. Hua, *Bioorg. Med. Chem. Lett.*, 2013, **23**, 6317–6320.
- 37 Y. Zhai, Y. Ma, F. Ma, Q. Nie, X. Ren, Y. Wang, L. Shang and Z. Yin, *Eur. J. Med. Chem.*, 2016, **124**, 559–573.
- 38 E. Arutyunova, M. B. Khan, C. Fischer, J. Lu, T. Lamer, W. Vuong, M. J. van Belkum, R. T. McKay, D. L. Tyrrell, J. C. Vederas, H. S. Young and M. J. Lemieux, *J. Mol. Biol.*, 2021, **433**(13), 167003.
- 39 A. S. Kalgutkar, K. S. Frederick, J. Chupka, B. Feng, S. Kempshall, R. J. Mireles, K. S. Fenner and M. D. Troutman, *J. Pharm. Sci.*, 2009, **98**(12), 4914–4927.
- 40 Vero E6 cells treated with 0.5 μ M CP in the absence of compound showed high viability (>80%) after 24 h using both CCK8 and CellTitreGlo determinations. The viability of Vero E6 cells in the presence 0.5 μ M CP and 18a–18c and 19b at 50 μ M and 200 μ M was also determined. The viability of the Vero E6 cells by CCK8 and CellTitreGlo for these compounds was lower than without CP, but was still above 50% at 200 μ M ($CC_{50} > 200 \mu$ M).
- 41 M. L. Biniössek, D. K. Nägler, C. Becker-Pauly and O. Schilling, *J. Proteome Res.*, 2011, **10**, 5363–5373.
- 42 C. P. Tinworth and R. J. Young, *J. Med. Chem.*, 2020, **63**, 10091–10108.
- 43 R. Brown, S. Nath, A. Lora, G. Samaha, Z. Elgamal, R. Kaiser, C. Taggart, S. Weldon and R. Geraghty, *Respir. Res.*, 2020, **21**, 111.
- 44 T. Liu, S. Luo, P. Libby and G.-P. Shi, *Pharmacol. Ther.*, 2020, **213**, 107587.
- 45 A. Pišlar, A. Mitrović, J. Sabotič, U. P. Fonović, M. P. Nanut, T. Jakoš, E. Senjor and J. Kos, *PLoS Pathog.*, 2020, **16**(11), e1009013.
- 46 C. P. Gomes, D. E. Gernandes, F. Casimiro, G. F. da Mata, M. T. Passos, P. Varela, G. Matroiani-Kirsztajn and J. B. Pesquero, *Front. Cell. Infect. Microbiol.*, 2020, **10**, 589505.
- 47 T. J. Cross, G. R. Takahashi, E. M. Diessner, M. G. Crosby, V. Farahmand, S. Zhuang, C. T. Butts and R. W. Martin, *Biochemistry*, 2020, **59**(39), 3741–3756.